An Inverse Design of an Open, Head/Neck RF Coil for MRI

Ben G. Lawrence*, Stuart Crozier, *Member, IEEE*, Gary Cowin, and Desmond D. Yau

***Abstract*—Radio-frequency (RF) coils are a necessary component of magnetic resonance imaging (MRI) systems. When used in transmit operation, they act to generate a homogeneous RF magnetic field within a volume of interest and when in receive operation, they act to receive the nuclear magnetic resonance signal from the RF-excited specimen. This paper outlines a procedure for the design of open RF coils using the time-harmonic inverse method. This method entails the calculation of an ideal current density on a multipaned planar surface that would generate a specified magnetic field within the volume of interest. Because of the averaging effect of the regularization technique in the matrix solution, the specified magnetic field is shaped within an iterative procedure until the generated magnetic field matches the desired magnetic field. The stream-function technique is used to ascertain conductor positions and a method of moments package is then used to finalize the design. An open head/neck coil was designed to operate in a clinical 2T MRI system and the presented results prove the efficacy of this design methodology.**

***Index Terms*—Electromagnetic, Green's function, inverse technique, magnetic resonance imaging, MRI, planar, RF coil.**

I. Introduction

THE inverse approach has been used to design gradient coils [1] and extended to the design of cylindrical radio-frequency (RF) coils first by the quasi-static approach [2]and later by the time-harmonic approach [3]. This paper outlines the design of an open RF coil using the time-harmonic inverse approach, as an extension to and modification of the technique outlined in [3].

This method entails the calculation of an ideal current density on an arbitrary planar surface that would generate a specified magnetic field. Because of the averaging effect of the regularization technique used in the matrix solution, the specified magnetic field is shaped within an iterative procedure until the generated magnetic field matches the desired magnetic field that, in this case, is a field of homogeneous magnitude. The stream-function technique is used to ascertain conductor positions and a method of moments package is then used to finalize the design.

The most common RF coil for volume imaging in magnetic resonance imaging (MRI) is the RF birdcage coil which encloses the imaged volume allowing open access from the top and bottom sides. To allow greater access to the imaged volume, it would be advantageous to design an RF coil with more open sides, such as in front as well as top and bottom. This also allows the coil to be placed in a closer vicinity to the imaged volume without making the subject feel claustrophobic. As a test for the methodology outlined in this paper, an open head/neck coil was designed to operate in a clinical 2T MRI system.

There have been a number of open RF coils designed in recent years. Open birdcage coils have been designed by breaking the two end-rings at the zero current points and then using half of the coil to generate the magnetic field [4], [5]. A U-shaped coil was also investigated for the different directional modes using the half-birdcage principle [6]. Alternatively, dome-shaped RF coils have been designed to enclose only the top half of the imaged volume using a mesh configuration [7], [8]. The design approach used in this paper differs from previous designs by using a modification of the time-harmonic inverse approach to calculate the current required to generate the specified field. A protoype was designed and constructed and the MRI results are presented herein.

II. Method

A. Current Density Basis Functions

The current on the surface of the geometry is described by a suitable set of basis functions. The choice of these basis functions is up to the designer, but in this paper, the geometry is essentially mapped onto a two-dimensional (2-D) surface on which the current basis functions are described with sinusoidal functions. In [9], however, pyramidal basis functions were used with the quasi-static approach.

The open head/neck coil geometry is shown in Fig. 1 with length L, width W and height H. The direction indicated by the z axis is the direction of the static $\mathbf{B}_0$ magnetic field. The current density on the surface can be split into two components: that current in the z direction and that current in the xy plane. If the latter current component direction is described with the variable v in the direction $\hat{\mathbf{v}}$ defined as in x direction on plate 1, in the y direction on plate 3 and in the $-x$ direction on plate 2, then the current components can be described by a general Fourier series

$$\mathbf{J}_z = \sum_{q=0}^{1}\sum_{p=0}^{1}\sum_{n=1}^{N}\sum_{m=1}^{M} c_{mnpq}\sin\left(k_n v + \frac{q\pi}{2}\right) \times \sin\left(k_m z + \frac{p\pi}{2}\right)\hat{\mathbf{z}} \quad (1)$$

Manuscript received October 22, 2001; revised February 13, 2002. This work was supported in part by the Australian Research Council. *Asterisk indicates corresponding author.*

*B. G. Lawrence is with the Redfern Integrated Optics Pty. Ltd., 1 Central Ave, Sydney 2016, Australia (e-mail: ben.lawrence@cmr.uq.edu.au).

S. Crozier is with The School of Information Technology and Electrical Engineering, University of Queensland, St. Lucia, Brisbane Q4072, Australia.

G. Cowin and D. D. Yau are with the Centre for Magnetic Resonance, University of Queensland, St Lucia, Brisbane 4072, Australia.

Publisher Item Identifier 10.1109/TBME.2002.802054.

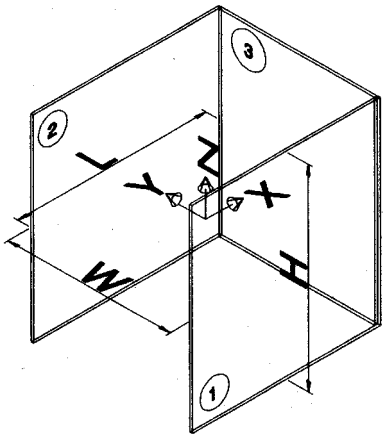

Fig. 1. The structure of the open planar head coil.

$$\mathbf{J}_v = \sum_{q=0}^{1}\sum_{p=0}^{1}\sum_{n=1}^{N}\sum_{m=1}^{M} a_{mnpq}\cos\left(k_n v + \frac{q\pi}{2}\right) \times \cos\left(k_m z + \frac{p\pi}{2}\right)\hat{\mathbf{v}} \tag{2}$$

where

$$k_m = \frac{m\pi}{H}$$

and

$$k_n = \frac{n\pi}{W+2L}$$

and the complex coefficients a_{mnpq} and c_{mnpq} are to be calculated.

B. Stream Functions

The $\hat{\mathbf{z}}$ and $\hat{\mathbf{v}}$ sinusoidal terms spatially differ by 90° because this form gives a convenient description of the scalar functions ψ and χ that fully describe the current density $\mathbf{J}$

$$\mathbf{J} = \hat{\mathbf{u}} \times \nabla\chi + \nabla\psi \tag{3}$$

where $\hat{\mathbf{u}}$ denotes the normal to the directions $\hat{\mathbf{v}}$ and $\hat{\mathbf{z}}$. In this report, ∇ is the 2-D differential operator with respect to $\hat{\mathbf{v}}$ and $\hat{\mathbf{z}}$ directions, that is

$$\nabla\chi \triangleq \hat{\mathbf{v}}\frac{\partial\chi}{\partial v} + \hat{\mathbf{z}}\frac{\partial\chi}{\partial z}$$

and

$$\hat{\mathbf{u}} \times \nabla\chi = -\hat{\mathbf{v}}\frac{\partial\chi}{\partial z} + \hat{\mathbf{z}}\frac{\partial\chi}{\partial v}.$$

Hence, the scalar function χ is conveniently expressed as

$$\chi = \sum_{q=0}^{1}\sum_{p=0}^{1}\sum_{n=1}^{N}\sum_{m=1}^{M} d_{mnpq}\cos\left(k_n v + \frac{q\pi}{2}\right) \times \sin\left(k_m z + \frac{p\pi}{2}\right). \tag{4}$$

The coefficients d_{mnpq} can be found in terms of the current coefficients a_{mnpq} and c_{mnpq}

$$d_{mnpq} = -\frac{c_{mnpq}k_n + a_{mnpq}k_m}{k_n^2 + k_m^2}. \tag{5}$$

Similarly, the divergence term can be expressed with

$$\psi = \sum_{q=0}^{1}\sum_{p=0}^{1}\sum_{n=1}^{N}\sum_{m=1}^{M} f_{mnpq}\sin\left(k_n v + \frac{q\pi}{2}\right) \times \cos\left(k_m z + \frac{p\pi}{2}\right) \tag{6}$$

where

$$f_{mnpq} = \frac{c_{mnpq}k_m - a_{mnpq}k_n}{k_n^2 + k_m^2}. \tag{7}$$

In this paper, as with [3], the coil current is preset with zero divergence so

$$c_{mnpq} = \frac{k_n a_{mnpq}}{k_m}. \tag{8}$$

There are many solutions of current distribution that will produce the required magnetic field. The important issue is to choose the current distribution that will readily lend itself to implementation in the form of conducting paths. After testing numerous solutions, it was found that for this case, the best choice is to have $\mathbf{J}_v = 0$ at the protruding edge $(v = \pm(L + W/2))$ of each of plates 1 and 2 (see Fig. 1) but allowing $\mathbf{J}_v \neq 0$ at the joining edges $(v = \pm W/2)$ of plates 1 and 3 and of plates 2 and 3. The current distribution also has $\mathbf{J}_z \neq 0$ at the top and bottom edges $(z = \pm H/2)$ of all the plates. This means $p = q = 1$ and $n = 2, 4, 6, \ldots, 2N$. The basis functions then reduce to

$$\mathbf{J}_z = \sum_{n=1}^{N}\sum_{m=1}^{M} \frac{k_n a_{mn}}{k_m}\cos(k_n v)\cos(k_m z)\hat{\mathbf{z}} \tag{9}$$

$$\mathbf{J}_v = \sum_{n=1}^{N}\sum_{m=1}^{M} a_{mn}\sin(k_n v)\sin(k_m z)\hat{\mathbf{v}} \tag{10}$$

where

$$k_m = \frac{m\pi}{H} \text{ and } k_n = \frac{n\pi}{W}.$$

The stream function simplifies to

$$\chi = \sum_{n=1}^{N}\sum_{m=1}^{M} \frac{a_{mn}}{k_m}\sin(k_n v)\cos(k_m z). \tag{11}$$

C. Magnetic Field Specification

The time-harmonic Green's function for free space is used to relate the current on an arbitrary surface to the magnetic field via the magnetic vector potential $\mathbf{A}$

$$\mathbf{A}(\mathbf{r}) = \frac{1}{4\pi}\int_{S_0} \mathbf{J}(\mathbf{r}')\frac{e^{-jk|\mathbf{r}-\mathbf{r}'|}}{|\mathbf{r}-\mathbf{r}'|}ds \tag{12}$$

where S_0 is the surface of the plate and the $\mathbf{J}(\mathbf{r}')$ is the surface current density.

Because it is the magnetic field that is specified and not its vector potential, the above equation should be rewritten in terms of the magnetic components. For the x component

$$B_x = \frac{\partial A_z}{\partial y} - \frac{\partial A_y}{\partial z}. \tag{13}$$

The differential operators in (13) are with respect to the point $\mathbf{r}$ of the field within the volume whereas the integral of (12) is

with respect to the point $\mathbf{r}'$ of the current on the surface, so the differential operators may be taken inside the integral sign [4]

$$B_x(\mathbf{r}) = \int_{S_0} \frac{\partial}{\partial y}\left(\frac{e^{-jkR}}{4\pi R}\right) J_z(v_0, z_0)ds - \int_{S_0} \frac{\partial}{\partial z}\left(\frac{e^{-jkR}}{4\pi R}\right) J_y(v_0, z_0)ds \quad (14)$$

where R is the distance from the specified point to a point on the current surface

$$R = \sqrt{(x-x_0)^2 + (y-y_0)^2 + (z-z_0)^2} \quad (15)$$

(x, y, z) denotes a point in space and (x_0, y_0, z_0) and denotes a point on the current density surface.

Equation (14) becomes

$$B_x = \int_{S_0} \frac{e^{-jkR}}{4\pi R^2}\left(jk + \frac{1}{R}\right) \times \left[-J_z(v_0, z_0)(y-y_0) + J_y(v_0, z_0)(z-z_0)\right] ds. \quad (16)$$

Similarly

$$B_y = \int_{S_0} \frac{e^{-jkR}}{4\pi R^2}\left(jk + \frac{1}{R}\right) \times \left[J_z(v_0, z_0)(x-x_0) - J_x(v_0, z_0)(z-z_0)\right] ds \quad (17)$$

$$B_z = \int_{S_0} \frac{e^{-jkR}}{4\pi R^2}\left(jk + \frac{1}{R}\right) \times \left[J_x(v_0, z_0)(y-y_0) - J_y(v_0, z_0)(x-x_0)\right] ds. \quad (18)$$

The current density is a surface current density and this is considered when taking the integral in the above equations.

The current density $\mathbf{J}$ can now be approximated with the set of basis functions (9) and (10), and substituted into the field (16)–(18). The number of equations that result corresponds to the number of designated points within the volume where the $\mathbf{B}$ field is specified.

D. Current Density Solution

The problem is to calculate a current density on the surface of the coil in Fig. 1 such that a relatively homogeneous field is generated perpendicular to the $\mathbf{B}_0$ field in the z direction. Current patterns were investigated that generate a homogeneous B_x field but these were not as practical to implement as those that generate a homogeneous B_y field. Hence, the basis functions of (9) and (10) are substituted into the field (17). This is then integrated over the coil surface to produce a matrix equation whose unknowns are the coefficients a_{mn} and c_{mn}.

If (a) denotes the column vector of the J_v coefficients, (c) denotes the column vector of the J_z coefficients, and $[\,]$ denotes a matrix, then the field in the diameter of the sensitive volume (DSV) due to the coil currents is found using (17). In matrix form, this is

$$[A](a) + [B](c) = (B_y) \quad (19)$$

where (B_y) is the column vector of the specified magnetic field at the designated points within interior region. $[A]$ and $[B]$ are the rectangular matrices resulting from numerically integrating (17).

As stated previously, the zero divergence condition (8) is imposed on the coil currents allowing the coil current to have only a rotational component which means the number of unknown coil coefficients is halved

$$[A'](a) = (B_y) \quad (20)$$

where $[A']$ is the combination of $[A]$ and $[B]$ of (19) using the relationship of (8).

The matrix (20) is usually not square because the number of points where the magnetic field is specified does not equal the number of unknown coefficients. The rank of the matrix is usually less than the number of unknown coefficients as well, and so a regularization method must be used for a solution.

1) Regularization: The method chosen was to minimize some functional in terms of the current density and impose the extra conditions onto the matrix (20). Numerous functionals are available and it is convenient to choose a functional such that the resulting current density is easiest to implement. This has been previously discussed in [3]. The functional

$$\min \int_{S_0} \mathbf{J} \cdot \mathbf{J} ds \quad (21)$$

results in a current density similar to one of minimum power and, hence, is an obvious choice. When the current density (9) and (10) is substituted into the above (21) and differentiated to find the coefficients for a minimum

$$\int_{S_0} \frac{\partial}{\partial a_{ij}}(\mathbf{J} \cdot \mathbf{J}) ds = 0. \quad (22)$$

The resulting matrix equation is just some constant multiplied by the identity matrix because the basis functions are orthonormal (to within a scalar independent of the basis function's order). The constant is taken into account by the value of the penalty variable so the regularization matrix $[R] = [I]$, $[I]$ being the identity matrix.

Solving the coefficients (a) is then a simple least squares problem

$$(a) = \left([A']^T[A'] + \lambda[R]\right)^{-1}[A']^T(B_y) \quad (23)$$

where λ is a scalar penalty variable to be chosen according to a number of factors. That is, λ should be a small as possible such that

- the matrix problem (23) is well-behaved.
- the error between the resulting field and the specified field (B_y) is within acceptable limits.
- the curvature of the contours of the resulting stream function χ is practical to implement into conductors.

E. Iterative Solution of the Desired Field

The magnetic field is specified in the field (17) in terms of the surface current. However, the least-squares method (23) for the matrix solution of (20) has the tendency to produce a solution such that the least squares error is minimized for a particular value of λ. The error of the field generated from the current solution will increase as λ increases. This error also tends to increase in the case of asymmetric geometries since the field points of (B_y) will be closer to certain regions of the coil's surface than to other regions, tending to increase those particular values of the matrix $[A']$ and consequently giving them more weight in the solution of (23). This means that the solution may not be such that the field it generates is closest to the desired field.

To compensate for these factors, the specified field in (B_y) is shaped to produce a field closest to the desired field.[1] The method then involves the following iterative procedure:

The current density is first calculated from (23). This current is then approximated by Hertzian dipoles and the resulting field calculated by the method of moments (MoM) package feko [10]. The field vector (B_y) is then compensated in the region where the field generated from feko fails to be homogeneous

$$\left(B_y'\right) = [\mathrm{diag}(P)](B_y) \tag{24}$$

$[\mathrm{diag}(P)]$ is a square matrix with a nonzero main diagonal chosen such that the field at a point p is multiplied by a value of the order $B_{yp}/B_{yp}^{\mathrm{MoM}}$ where B_{yp} is the specified y directed magnetic field at point p and B_{yp}^{MoM} is the resulting magnetic component after the initial currents were simulated with the MoM package. It was found that the specified field needed to be reshaped and the currents recalculated a number of times because changing the specified field at a single point affects the resulting field in all the region, as can be expected from a field satisfying Helmholtz equation. Then

$$(a) = \left([A']^T[A'] + \lambda[R]\right)^{-1}[A']^T\,[\mathrm{diag}(P)]\,(B_y). \tag{25}$$

In most cases, it is not sufficient just to approximate the current with Hertzian dipoles. It may well be that the device has to be simulated with conductors and a feed-point in order to ascertain where the field fails to meet the criterion. With this knowledge, the matrix $[\mathrm{diag}(P)]$ can be more accurately constructed.

The final current calculated will be the result of an iterative procedure of reshaping the specified field to obtain a satisfactory 'desired' field after simulation.

III. Implementation

To ascertain the efficacy of the methodology, a linear transmit/receive open head/neck coil was designed to operate at 85 MHz for a 2T magnet system. The initial dimensions were length $L = 350$ mm, $W = 300$ mm and $H = 400$ mm as shown in Fig. 1 for a DSV of around 200 mm. The basis functions (9) and (10) had dimensions of $M = 5$ and $N = 5$. The penalty value used in the matrix solution of (25) was $\lambda = 10$. The goal of the design was to generate a homogeneous coverage of head and neck while maintaining an open aspect in front of the face.

The first step in the design procedure is to calculate the current density that will generate a unitary (homogeneous) magnetic field using the above time-harmonic inverse method. The current density is then approximated by Hertzian dipoles in a method of moments (MoM) program (feko) and the magnetic field calculated. The specified field points for this case were arranged cylindrically, with three points in the radial direction, 16 in the phi direction (according to cylindrical coordinate system) and 12 in the z direction and 12 more along the z axis giving a total number of 584 equations, one for each specified point. These equations are put into matrix form and the least squared method with regularization (25) is applied.

Initially, the simulated magnetic field was not as desired, so the specified field in the inverse method was shaped and the current recalculated as per (25). The shaping used on a unitary B_y source field is shown in Fig. 2. Note that the field had to be compensated in the x direction away from plate 3, since initially, the magnetic field decreased unsatisfactorily in that direction. It was also found that the magnetic field intensity near plates 1 and 2 was too great initially, so compensation was needed to emphasize the central field along the y axis away from the side plates 1 and 2. The field was quite homogeneous in the z direction so little compensation was required.

Once a satisfactory magnetic field was generated from the current distribution, the stream function χ was calculated so that the contours of the stream-function χ are used as the positions of the wires. The real and imaginary components of χ are shown in Figs. 3 and 4, respectively. The maximum value of the real component of the current is about 30 times greater than the imagi-

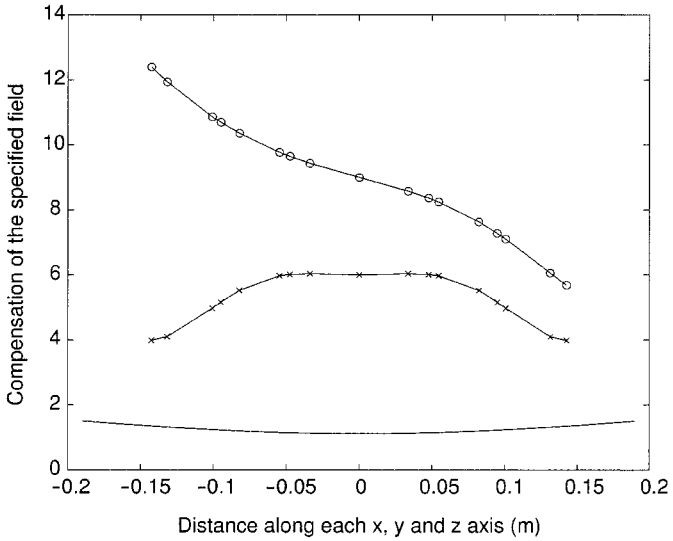

Fig. 2. The functions that are applied to the unitary y directed magnetic field B_y in order to generate a homogeneous field. The -o- line, the -x- line and the unmarked line represents the intensity of B_y' of (24) in the x axis, y axis and z axis, respectively.

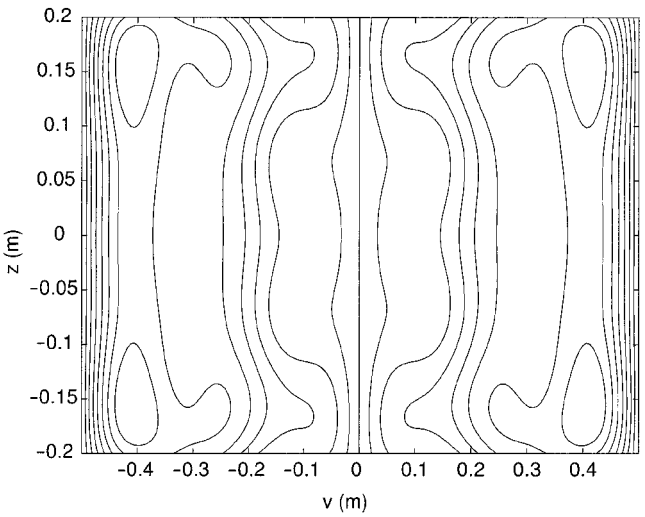

Fig. 3. The contours of χ for the real component of the vector current density. The coil is described with the variables z and v where v is in the direction $\hat{\mathbf{v}}$ defined as in x direction on plate 1, in the y direction on plate 3 and in the $-x$ direction on plate 2 (see Fig. 1).

[1]"Specified" field is that specified in the matrix problem of (23) whereas 'desired' field is the resulting homogeneous field in the DSV

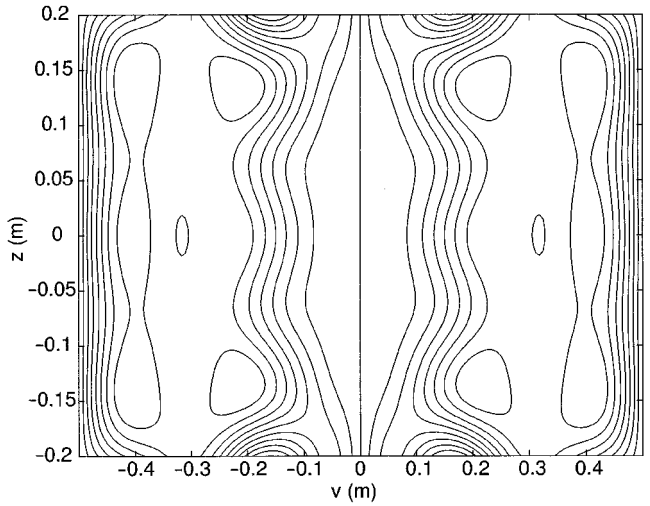

Fig. 4. The contours of χ for the imaginary component of the vector current density. This component is significantly less than the real component and so can be ignored in the implementation of the coil. The coil is described as in Fig. 3 .

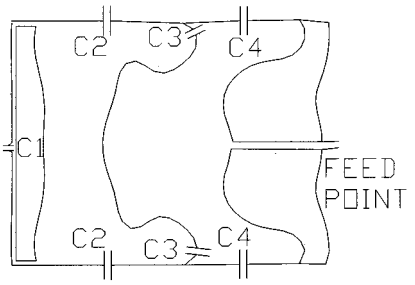

Fig. 5. One half of the circuit diagram designed from the contours of Fig. 3.

nary component and so the imaginary component could be reasonably ignored. However, as frequency of operation increases, so does the imaginary component and so both components will have to be taken into account for higher frequency designs.

The contours of Fig. 3 were used as a guide to the position of wires in a reasonable design. Specifically, the wires have to be connected together and there has to be a feed-point. Capacitors are also required to adjust the current level in the wires, initiate a resonant mode of operation and for tuning and matching purposes. One solution is shown in Fig. 5 and the corresponding feko model is shown in Fig. 6.

The wires are 2 mm in diameter and $C1 = 54$ pF, $C2 = 12$ pF, $C3 = 6.8$ pF and $C4 = 10$ pF following the same implementation procedure as [3]. This solution was obtained iteratively with the MoM program as well as lab-trials within the 2T MRI system. Modeling alone is not sufficient because the planar head coil is unshielded and the external environment affects the coil's resonant frequency. This environment includes such things as the whole body birdcage coil and its shield already present within the MRI machine.

IV. Results

The magnitude of the field along the x, y, and z axes is shown in Fig. 7 which are the results from feko simulation. The magnetic field had negligible z component. As can be seen, the coil

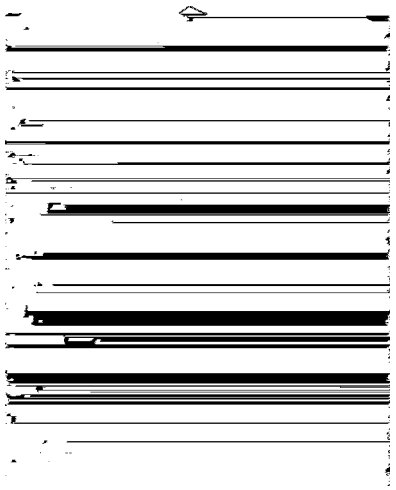

Fig. 6. The feko model for the open planar head coil corresponding to the circuit in Fig. 5.

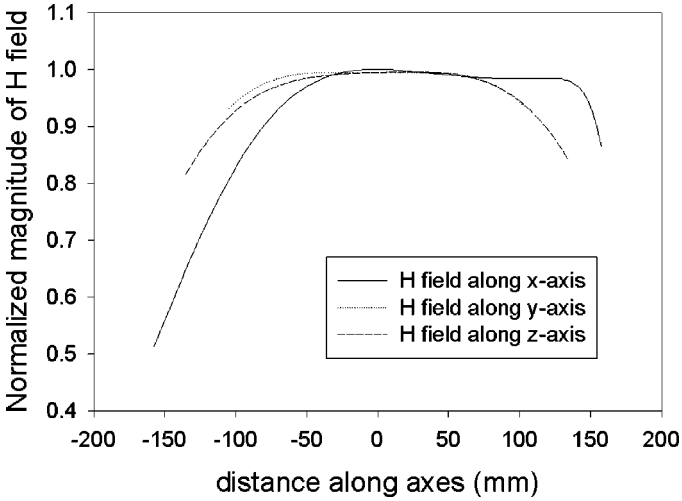

Fig. 7. The magnitude of the magnetic field along the x, y and z axes as simulated in feko.

gives a good DSV region of greater than 20 cm in diameter to within a 5% variation of the magnetic field.

The prototype coil was tested in transmit and receive operation even though it is envisaged to design receive-only coils as the final product. Images of a head and neck of one of the authors (B.L.) are shown in Figs. 8–10.

The gradient echo images were acquired on a 2T Bruker MRI system. In all cases a 256 square matrix was acquired. For the sagittal image of Fig. 8, TR/TE was 44.7/6.5 ms with a 40-cm field of view (FOV), a 5-mm slice thickness and a total image acquisition time of 45 s. For the transverse image in Fig. 9, TR/TE was 44.7/6.5 ms with a 26-cm FOV, a 5-mm slice thickness and a total image acquisition time of 45 s. For the transverse neck image in Fig. 10, TR/TE was 89/6.5 ms with a 20-cm FOV, a 5-mm slice thickness and a total image acquisition time of 93 s. Note the excellent homogeneity displayed in the images and in particular the large neck coverage down to the T2 vertebra shown in Fig. 8. This is further emphasized in Fig. 10 where a transverse image at the level of $C7$ shows good homogeneity and signal-to-noise ratio (SNR) for the coil. This is a particularly good result as the coil structure is completely open at the

Fig. 8. A sagittal image of a head and neck using the open head/neck coil.

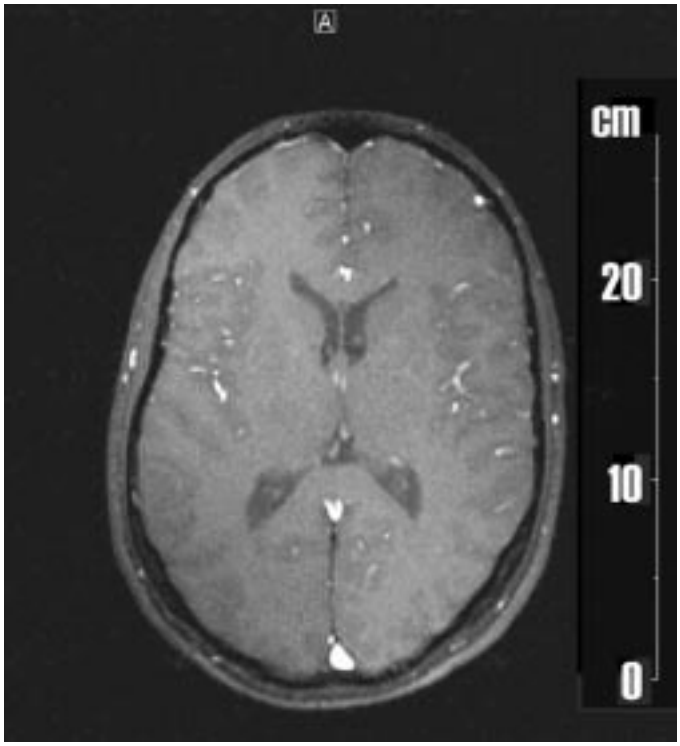

Fig. 9. An axial image of a head using the open head/neck coil.

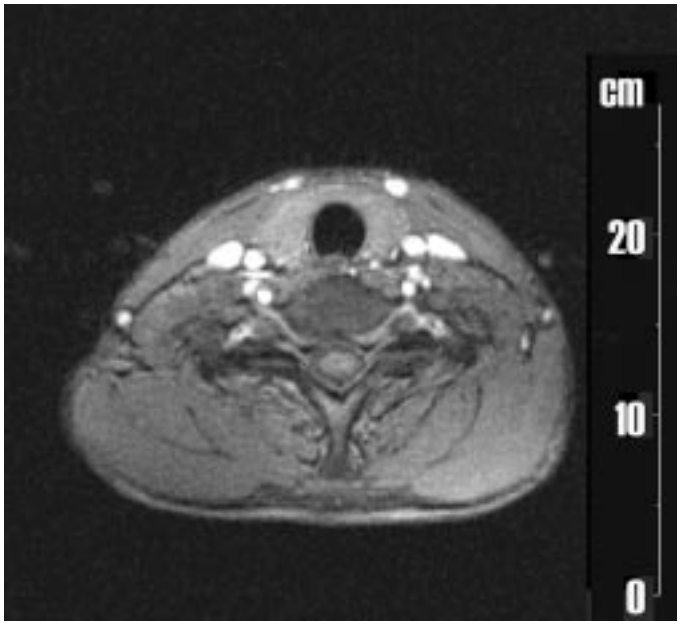

Fig. 10. A transverse image of the neck at the level of $C7$ using the open head/neck coil.

front giving the patient clear vision, an attribute expected to be useful for functional MRI studies. The bright spots in these figures indicate blood vessels.

Some comparisons with conventional coils is warranted. Although the authors do not have a birdcage head coil of the same size as the prototype, a smaller quadrature head coil was available for comparison. The linear open head/neck coil was tested in transmit/receive mode and compared with a setup where a whole-body birdcage was used in transmit mode and the smaller quadrature birdcage head-coil was used in receive mode. A 20-cm QA phantom was imaged for the purposes of comparing SNR and homogeneity. Given that the birdcage is smaller and used in quadrature, an SNR of about 1.8 times that of the prototype coil would have been expected, even though the smaller birdcage coil does not to have the same coverage or patient vision as the open head/neck coil. The results indicate an averaged SNR comparison (18 signal regions, six noise regions) of a ratio of approximately two. However, the homogeneity of the prototype head/neck coil was slightly better than its smaller birdcage counterpart.

In terms of the regulatory safety of the open head/neck coil, a human head model[2] with frequency dependent tissue properties (i.e., relative permittivity and conductivity) [11] was simplified to 1.5-cm size voxels and placed in the head/neck coil model in an MoM simulation. By comparing these simulated results with how much power was used in the actual test, it is estimated that in the head target, there was an average SAR of 0.1 W/kg with a maximum SAR of 2.9 W/kg.

[2]Available: ftp://starview.brooks.af.mil

V. Conclusion

To assist in the design of arbitrarily shaped RF coils, a methodology was presented that utilizes the time-harmonic inverse technique. The efficacy of the methodology was tested by designing an open head/neck coil to operate within a 2T clinical MRI system. The results presented show that a

practical receive-only head coil is possible, even though the initial prototype presented herein operated as a transmit and receive coil. Further work would be directed to improving the SNR of the coil.

ACKNOWLEDGMENT

The authors would like to thank S. Teed, J. Herriot, E. Weber, B. Beattie and other members of the CMR Engineering Facility for support and valuable assistance in the construction of the RF coil.

REFERENCES

[1] M. A. Martens, L. S. Petropoulos, R. W. Brown, and J. H. Andrews, "Insertable biplanar gradient coils for magnetic resonance imaging," *Rev. Sci. Instrum.*, vol. 62, no. 11, pp. 2639–2645, Nov 1991.

[2] H. Fujita, L. S. Petropoulos, M. A. Morich, S. M. Shvartsman, and R. W. Brown, "A hybrid inverse approach applied to the design of lumped-element RF coils," *IEEE Trans. Biomed. Eng.*, vol. 46, pp. 353–361, Mar. 1999.

[3] B. G. Lawrence, S. Crozier, D. Yau, and D. Doddrell, "A time-harmonic inverse methodology for the design of RF coils in MRI," *IEEE Trans. Biomed. Eng.*, pp. 64–71, Jan. 2002.

[4] J. Jin, *Electromagnetic Analysis and Design in Magnetic Resonance Imaging*. Boca Raton, FL: CRC, 1999.

[5] D. Ballon, M. C. Graham, S. Miodownik, and J. A. Koutcher, "A 64 MHz half-birdcage resonator for clinical imaging," *J. Magn. Reson.*, vol. 90, pp. 131–140, 1990.

[6] J. Gasson, I. R. Summers, M. E. Fry, and W. Vennart, "Modified birdcage coils for target imaging," *Mag. Reson. Imag.*, vol. 13, pp. 1003–1012, 1995.

[7] K. L. Zakian, J. A. Koutcher, and D. Ballon, "A dual-tuned resonator for proton-decoupled phosphorus-31 chemical shift imaging of the brain," *Magn. Reson. Med.*, vol. 41, no. 4, pp. 809–815, 1999.

[8] K. L. Meyer, K. Kim, T. Li, P. K. Tulipano, K. M. Lee, R. DeLaPaz, J. Hirsch, and D. Ballon, "Sensitivity-enhanced echo-planar MRI at 1.5 t using a 5×5 mesh dome resonator," *Magn. Reson. Med.*, vol. 36, no. 4, pp. 606–612, 1996.

[9] D. Yau, B. G. Lawrence, and S. Crozier, "A method for the design of MRI radiofrequency coils based on triangular and pulse basis functions," MAGMA, 2002, to be published.

[10] *Feko User's Manual*, 3.05 ed., EM Software & Systems, Stellenbosch, South Africa, 2001.

[11] C. Gabriel and S. Gabriel. (1996) Compilation of the dielectric properties of body tissues at RF and microwave frequencies. United States Air Force Research Laboratory. [Online]. Available: http://www.brooks.af.mil/AFRL/HED/hedr/reports/dielectric/home.html Tech. Rep. AL/OE-TR-1996-0037.

Ben G. Lawrence received the B.Eng. degree from James Cook University, Queensland, Australia, and the Ph.D. degree for his dissertation, "Three dimensional finite element analysis of passive microwave devices," from Monash University Melbourne, Australia.

He worked with the Centre of Magnetic Resonance at University of Queensland as a Postdoctoral Research Fellow for two years since January 2000 and is now involved in designing electro-optical modulators for Redfern Integrated Optics Pty Ltd., Sydney, Australia. His chief interests are electromagnetics, magnetic resonance technology, and microwave integrated circuits.

Stuart Crozier (M'93) received the Ph.D. and D.Eng. awards from The University of Queensland, Queensland, Australia, in 1991 and 2002, respectively.

He currently holds the position of Professor of Biomedical Engineering in The School of Information Technology and Electrical Engineering, UQ. He has published over 90 journal articles and patents. His major research interests include magnetic resonance engineering and the methodological development of magnetic resonance.

Gary Cowin received the B.Sc. degree (with honors) from the University of New England, Biddeford, ME, and the Ph.D. degree from the University of Queensland, Queensland Australia.

He is currently a Research Officer at the Centre for Magnetic Resonance, University of Queensland. His research interests include *in vivo* applications of magnetic resonance spectroscopy and QA analysis of MRI systems.

Desmond D. Yau received the B.E. degree in electrical engineering from the University of Sydney, Sydney, Australia, in 1988, and the M.Eng.Sc. and Ph.D. degrees in electrical engineering from the University of Queensland, Queensland, Australia, in 1997 and 2001, respectively.

He is currently working with the Centre for Magnetic Resonance, University of Queensland. His research interest includes magnetic resonance imaging radio-frequency coil design, computation electromagnetic, and modeling of microwave antennas and guided structures.